

OQAM based Bi-orthogonal 5G System for IoT Device Communications

Ravi Sekhar Yarrabothu
Department of ECE,
Vignan's Foundation for Science Technology and Research,
Vadlamudi, India
yk ravi@gmail.com

Prithiviraj Venkatapathy,
Department of ECE,
Vignan's Foundation for Science Technology and Research,
Vadlamudi, India
profvp raj@gmail.com

Abstract — The recent advances in wireless technologies made it possible to inter connect every device wirelessly to the Internet, which is called as Internet of Things (IoT). 5G cellular communication research community has been compelled to design solutions for the IoT along with conventional data communications and voice/video over IP networks. The IoT plays a critical role in the modern society with smart cities, smart power grids and other applications. These applications demand ultra low power and low cost solutions. To meet such diversified requirements, novel physical layer need to be designed. In this paper, a novel accessing technique with the LTE procedures defined by 3GPP has been used to cater the needs of IoT devices generated random traffic. A new system with Offset Quadrature Amplitude Modulation (OQAM) and bi-orthogonal frequency division multiplexing (BFDM) is simulated using Matlab Software along with BFDM QAM and LTE based OFDM. In this paper, the performance of BFDM-OQAM system is compared with OFDM and BFDM QAM systems under Line of Sight fading conditions such as Rural Line of Sight (RLOS), Highway Line of Sight (HLOS), and Urban Approaching Line Of Sight (UALOS).

Keywords— BFDM, HLOS, IoT, LTE, MTC, OFDM, OQAM, RLOS, UALOS, 3GPP, 5G

I. INTRODUCTION

The evolution of Internet of Things (IoT) has been instrumental in changing our daily life beyond our imagination and is the stepping stone for 5G. 5G Research is driven by the Machine-to-Machine (M2M) communication, ubiquitous broadband connectivity, and the tactile internet. The Internet of Things (IoT) would be the predominant driver for the 5G cellular communication networks [1] growth. The reach of IoT spans across every area of lifestyle and business providing the advantages of improved customer engagement, optimization of resources, enhanced connectivity, and efficient data collection from various sources on continuous basis. Efficient access to the 5G networks for the random traffic generated by these IoT devices is a bigger challenge since these are inactive for longer durations and the periodic internet access is done for trivial or incremental update without human intervention. In 5G networks, hundreds of interconnected IoT devices will be a norm and handling such an exponential growth of sporadic traffic with the existing LTE random access procedures is a herculean task.

In this paper, a novel method [2],[3] has been applied to handle proficiently such a bursty natured 5G traffic with an improved Physical Random Access Channel (PRACH), which accomplish simultaneous device synchronization and small data payload transmission. In LTE, scalability of the

sporadic traffic is not possible due to the reason that only consumer data is carried by the Physical Uplink Shared Channel (PUSCH). In 3GPP Release 13, few enhancements for physical layer [4] are proposed for enhanced Machine Type Communications (eMTC). A new design of Data PRACH (D-PRACH) is introduced for supporting asynchronous data transmission [2] by positioning a data access part between the PRACH and synchronization PUSCH. The so called D-PRACH uses the guard band between PUSCH. By doing so, asynchronous bursty traffic is left out from the uplink shared channel PUSCH and signaling overhead is been drastically reduced, which translates in to reasonably good power saving for the IoT devices. The guard bands scarifying for the sake of data transmission, usually lead to interference amplification for PUSCH users, but the design of newer waveform BFDM takes care of it.

In BFDM, simple orthogonality is substituted with pair wise orthogonal set of transmit and receives pulses. As a result of this, more freedom is acquired for the transmit pulse prototype design with very good side lobe suppression. For BFDM detection Matched filters are not appropriate and in this work a Zero Forcing (ZF) filter is used [5]. The transmission of PRACH symbols in BFDM system is highly resistant to timing offsets and is much suitable for asynchronous sporadic data transmission. BFDM with OQAM shows greater robustness to Doppler shifts of the signal due to the channel environment, when compared to conventional OFDM systems. In 5G communications, massive machine communication is a vital requirement for its success and this can be fulfilled by using the BFDM-OQAM system.

In this paper, the work carried out is presented in five sections. Firstly the section II, design details of the BFDM system is discussed and section III explains about the necessity of BFDM-OQAM. The system simulation of BFDM and OFDM based systems are talked in section IV and the simulation results are presented in section V. Finally, the conclusions and future scope of the work are talked in section VI.

II. DESIGN OF BFDM SYSTEM

Similar to OFDM systems, the PRACH transmission goes through pulse shaping technique in the BFDM system. The transmitted symbols are as per a group of time and frequency shifted pulses with the lattice points $((kT, lF))$, where T and F are time domain and frequency domain shifts respectively. As stated in [2], the precise symbol reconstruction can be

achieved only if the transmit pulses $\{g_{k,l}\}$ and the receive pulses $\{\gamma_{k,l}\}$ form the bi-orthogonal Riesz bases. Perfect reconstruction of symbols is determined by two features i.e. pulse properties and the time-frequency product $TF (>1)$, where symbol duration is T , and subcarrier frequency spacing is F . In the current work $TF=1.25$ is chosen which found to be optimum.

A. Transmitter

The PRACH transmitter is as shown in the figure 1, with an additional process to the pulse shaped PRACH [6], compared to normal OFDM. Here shaping of the PRACH signal is performed by the pulse 'g', which is based on the B-Spline. The primary reason for using the B-Spline pulses is due to its excellent tail properties. In figure 1, the data after sub carrier mapping, IFFT is applied, stacked as a row matrix, then convoluted with the time shifted pulse 'g', and laid over by overlapping and adding to get the pulse shaped PRACH signal.

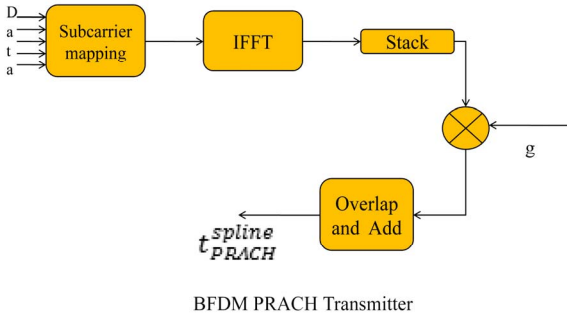


Figure 1 PRACH transmitter for BFDm [2]

Shaping of the PRACH signal spectrum is done by using a pulse g. Let 'P' be the length of pulse g. The transmitted signal $t[n]$ generated after the inverse FFT (IFFT) stage by iterating and taking modulo P, which is of same length P. Given k symbols, each symbol $t_k[n]$ is stacked as row matrix

$$T = \begin{pmatrix} t_0[n] \\ t_1[n] \\ \vdots \\ t_{K-1}[n] \end{pmatrix}, S \in \mathbb{C}^{K \times P} \quad (1)$$

Each $t_k[n]$ is point wise multiplied with the shifted pulse g and superimposed by overlap and add. Then, the base band pulse shaped PRACH transmit signal is

$$t_{pr}^{ps}[n] = \sum_{k=0}^{K-1} t_k[n]g[n - kN] \quad (2)$$

B. Receiver

Pulse shaped receiver for PRACH channel is as shown in figure 2. First an inversion operation is carried out on the transmitter side pulse. Here the first K symbols of the received signal $o_{PR}[n]$ are arranged in a row vector matrix.

$$O = \begin{pmatrix} o_0[n] \\ o_1[n] \\ \vdots \\ o[n] \end{pmatrix}, R \in \mathbb{C}^{K \times P} \quad (3)$$

Then each row is multiplied point wise by the shifted bi-orthogonal pulse γ , so the received signal is

$$o_k^{\gamma}[n] = o_k[n]\gamma[n - kN] \quad (4)$$

In figure 2, received PRACH signal is stacked, convoluted with the pulse γ , which is a canonical dual (bi-orthogonal) of the transmitted pulse 'g'. Then FFT is applied on the received output and sub carrier demapping is done to get the output data at the BFDm receiver.

Pulse shaping is designed as mentioned in [8] and [9] for both transmitter and receiver of BFDm PRACH channel. The BFDm system design is explained in more detailed in [10] and [11].

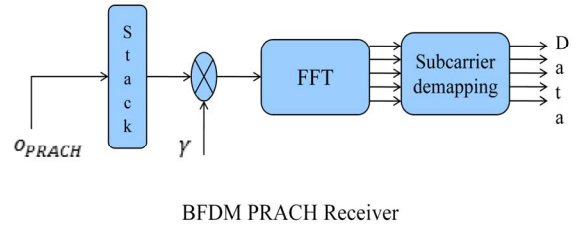


Figure 2 PRACH Receiver of BFDm [2]

III. OQAM BASED BFDm SYSTEM

In the Offset QAM, real and imaginary parts of a complex data symbol are not transmitted simultaneously as it happens in QAM. The imaginary part of the complex symbol is transmitted with a half symbol delay. Since real and imaginary are half the inverse of the sub-channel spacing apart in time domain, the word "offset" is justified. Figure 3 illustrates the distinction between QAM and OQAM modulations [12].

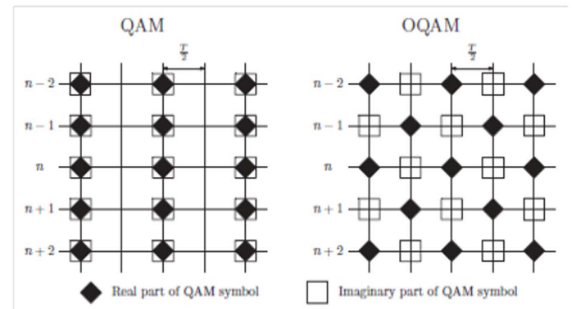


Figure 3 Representation of Symbol Transmission for QAM and OQAM

OFDM is based on the principle of strict orthogonality. However orthogonality restricts the achievable localization of time-frequency. So, relaxation of orthogonality is warranted and OQAM based BFDm significantly improve time-frequency localization, which translates in to improved spreading robustness.

IV. BFDm SYSTEM SIMULATION

A typical BFDm system is diagrammatically represented in figure 4. The block diagram consists of *Data Source*,

Encoder data, BFDM Modulator (BFDM Transmitter), Channel, BFDM Demodulator (BFDM Receiver), and Decoder. In figure 4, data from a source is encoded by using channel coding techniques, using a BFDM modulator converted to a BFDM signal for transmission through a channel. At the receiver, BFDM demodulator demodulates the received BFDM signal, and decoded in to data.

A. Channel

In digital communication, channel characterization is an important thing to find out the effectiveness of the wireless system. Channel modeling considers along with noise, fading of signal due to multi path is an important component. Over longer distances of signal travel, the degradation of the transmitted signal is known as fading. In general, fading channels are of two types: Non-Line of Sight (NLOS) and Line of Sight (LOS) and are modeled by Rayleigh distribution and Rician distribution respectively. In this paper, Rician distribution is used, since the MTC is mostly Line of Sight communication.

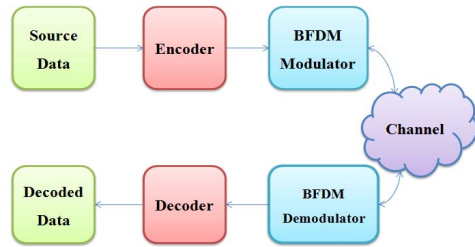


Figure 4 BFDM Transceiver block diagram

B. Multipath Fading Channels

When a signal propagates through a channel and reaches the receiver, from multiple paths apart from the direct path due to reflections, scattering and diffraction. In this work, three multipath fading channel models based on the appropriate Line of Sight conditions relevant for IoT devices are used namely RLOS, HLOS and UALOS [13], [14] and [15]. These fading profiles are the representation of low, medium, and high delay spreads respectively and is shown in the Table 1.

TABLE 1 LOS PROFILES

RURAL LINE OF SIGHT (RLOS) PROFILE			
Tap No	Excess tap delay (in Nano Seconds)	Relative Power (in dB)	Doppler Shift (in Hz)
1	0	0	0.0
2	83.0	-14.0	-492.0
3	180.0	10.0	-295.0
URBAN APPROACHING LINE OF SIGHT (UALOS) PROFILE			
Tap No	Excess tap delay (in Nano Seconds)	Relative Power (in dB)	Doppler Shift (in Hz)
1	0	0.0	0.0
2	117.0	-8.0	236

3	183.0	-10.0	-157
4	333.0	-15.0	492
HIGHWAY LINE OF SIGHT (HLOS) PROFILE			
Tap No	Excess tap delay (in Nano Seconds)	Relative Power (in dB)	Doppler Shift (in Hz)
1	0.0	0	0
2	100.0	-10.0	689.0
3	167.0	-15.0	-492.0
4	500.0	-20.0	886.0

V. SIMULATION RESULTS

In this paper, BFDM/OQAM, BFDM/QAM and OFDM/QAM systems with PRACH channel are simulated by using Matlab software. These systems are evaluated under various the 3GPP fading profiles defined in section IV. The simulation parameters used for the BFDM and OFDM systems are as shown in Table 2.

In the BFDM system, carrier spacing is reduced to 1.25KHz from 15 KHz, which is a defined in OFDM system. Figure 5 presents the Power spectral density (PSD) analysis for BFDM/OQAM, BFDM/QAM.

Table 2 Simulation parameters

S.No	Parameter	OFDM PRACH	BFDM PRACH
1	Bandwidth	1.08MHz	1.08MHz
2	Spacing between Subcarriers	1.25KHz	1.25KHz
3	Duration of OFDM symbol (Ts)	800μs	-
4	Length of FFT (NFFT)	24576	24576
5	Sampling rate	30.72MHz	30.72MHz
6	Number of subcarriers	839	839
7	Guard time	2976 * Ts	0
8	Cyclic prefix length	3168 * Ts	0
9	Number of Symbols	1	1
10	Pulse length	-	4ms
11	Channel Coding	Turbo	Turbo
12	Time-frequency product	1.25	1.25

From figure 5, one can detect that the side-lobes for BFDM systems is suppressed better than in OFDM system and the BFDM/OQAM system has much improved side lobe suppression than BFDM/QAM and OFDM system.

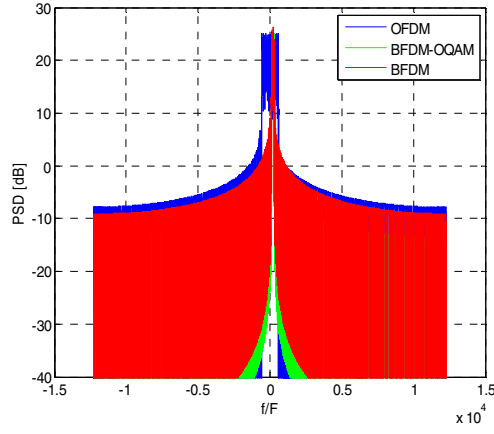


Figure 5 BFD and OFDM PSD Diagram

In this work, Symbol Error Rate (SER) analysis of BFD/OQAM, BFD/QAM and OFDM systems with various fading conditions are represented in figures 6, 7 and 8.

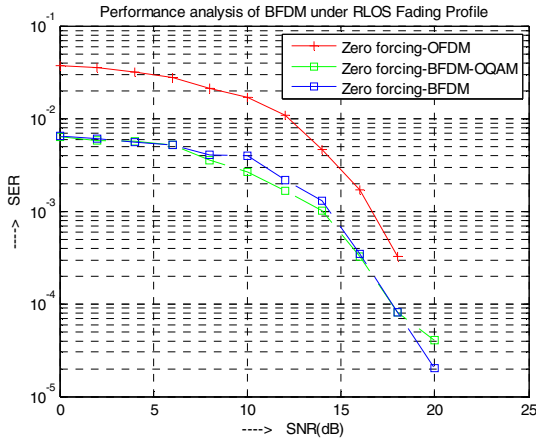


Figure 6 SER analysis for BFD, BFD-OQAM and OFDM systems under RLOS fading conditions

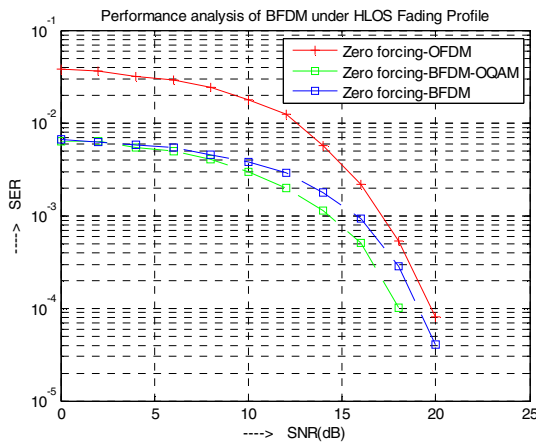


Figure 7 SER analysis for BFD, BFD-OQAM and OFDM systems under HLOS fading conditions

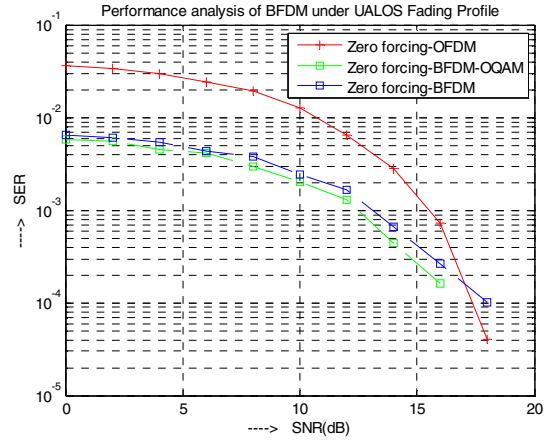


Figure 8 SER analysis of BFD, BFD-OQAM and OFDM systems under UALOS fading conditions

From the figures 6, 7 and 8, it can be noted that the SER for BFD system is better than the OFDM system under various LOS fading profiles. The BFD systems are more immune to frequency-time offsets and another interesting observation is BFD/OQAM system has better SER, under HLOS and UALOS fading profile conditions which has higher Doppler shift compared to RLOS profile.

As BFD systems are loosely synchronized and the time and frequency offset errors are minimum, BFD systems can be considered as very much appropriate for the rural and urban highway environments where huge number IoT devices will be interconnected and short messages are exchanged.

VI. CONCLUSION

In this work, it has been concluded that BFD systems perform better than the OFDM systems under various line of sight conditions. BFD is invulnerable to frequency and time offsets which are quite common in cellular communications and also more suited for MTC. The BFD/OQAM system is more impervious to real-time LOS fading conditions and in particular very much suitable for IoT kind of applications, where the deployments everywhere on the highways as well as remote rural areas. The OQAM based BFD system has very good side lobe suppression and it leads to device power saving, which is an essential thing for IoT applications, where thousands of IoT sensor devices are deployed in the fields. This OQAM based BFD can be very much suitable for 5G communications to fulfil one of its requirement of support for mass machine type communications. The presented work can be enhanced by introducing other pulse shapes like trapezoidal.

REFERENCES

- [1]. G. Wunder, P. Jung, M. Kasparick, T. Wild, F. Schaich, Y. Chen, S. ten Brink, I. Gaspar, N. Michailow, A. Festag, L. Mendes, N. Cassiau, D. Ktenas, M. Dryjanski, S. Pietrzyk, B. Eged, P. Vago, and F. Wiedmann, "5GNOW: Non-Orthogonal, Asynchronous Waveforms for Future Mobile Applications," IEEE Communications Magazine, vol.52,no. 2, pp. 97–105, 2014.
- [2]. M. Kasparick, G. Wunder, P. Jung and D. Maryopi, "Bi-orthogonal Waveforms for 5G Random Access with Short Message Support,"

European Wireless 2014; 20th European Wireless Conference, Barcelona, Spain, 2014, pp. 1-6

- [3]. G. Wunder, M. Kasparick, P. Jung, "Spline Waveforms and Interference Analysis for 5G Random Access with Short Message Support", Jan 15, 2015.
- [4]. A. Rico-Alvarino et al., "An overview of 3GPP enhancements on machine to machine communications," in IEEE Communications Magazine, vol. 54, no. 6, pp. 14-21, June 2016.
- [5]. W. Kozek and A. Molisch, "Nonorthogonal pulse shapes for multicarrier communications in doubly dispersive channels," IEEE Journal Sel. Areas in Communications, vol. 16, no. 8, pp. 1579-1589, 1998.
- [6]. D. Schafhuber, G. Matz, and F. Hlawatsch, "Pulse-shaping OFDM/BFDM systems for time-varying channels: ISI/ICI analysis, optimal pulse design, and efficient implementation," in 13th IEEE International Symposium on Personal, Indoor and Mobile Radio Communications, vol. 3, 2002, pp. 1012-1016 vol.3.
- [7]. P. Jung and G. Wunder, "The WSSUS Pulse Design Problem in Multicarrier Transmission," IEEE Trans. on Communications, 2007
- [8]. I. Daubechies, "Ten Lectures on Wavelets," Philadelphia, PA: SIAM, 1992.
- [9]. V. D. Prete, "Estimates, decay properties, and computation of the dual function for Gabor frames," Journal of Fourier Analysis and Applications, 1999.
- [10]. Ravi Sekhar Yarrabothu, Usha Rani Nelakuditi, "Performance analysis of Bi-orthogonality Based Systems for 5G Internet of Machine Critical Things Communications", International Journal of Simulation Systems, Science & Technology, Publication of United Kingdom Simulation Society, February 2018.
- [11]. Ravi Sekhar Yarrabothu, Sivaji Satrasupali, Lakshmi Gutha, "Performance Analysis of 5G Waveform – Bi-Orthogonal Frequency Division Multiplexing under Real Fading Condition Simulations", International Journal of Engineering & Technology, Volume 7(4.5), 2018 pp. 175-178.
- [12]. Qinwei He, AnkeSchmeink, "Comparision and Evaluation between FBMC and OFDM systems", WSA 2015, March 3-5, 2015, Ilmenau, Germany.
- [13]. Evolved Universal Terrestrial Radio Access (E-UTRA); Base Station (BS) radio transmission and reception (3GPP TS 36.104 version 11.2.0 Release 11)
- [14]. Clerckx B, Lozano A, Sesia S, van Rensburg C and Papadis B. 3GPP LTE and LTE Advanced. EURASIP J. Wireless Commun. Netw. Sep 2009;1: 472-124.
- [15]. Maddah-Ali M, Motahari A, Khandari A. Communication over MIMO X channels: Interference alignment, decomposition, Performance analysis. IEEE Trans. Inf. Theory; Aug 2008;54:3457-3470.